Functional analysis of the polycomb-group gene *Pcgf5* in hematopoietic stem and progenitor cells

（ポリコーム群遺伝子*Pcgf5*の造血幹・前駆細胞における機能解析）

千葉大学大学院医学薬学府

先端医学薬学専攻

（主任：岩間　厚志教授）

司　沙

Abstract

Polycomb-group RING finger proteins (Pcgf1-Pcgf6) are components of Polycomb repressive complex 1 (PRC1)-related complexes that catalyze monoubiquitination of histone H2A at lysine 119 (H2AK119ub1), an epigenetic mark associated with repression of genes. Pcgf5 has been characterized as a component of PRC1.5, one of the non-canonical PRC1, consisting of Ring1a/b, Rybp/Yaf2 and Auts2. However, the biological functions of Pcgf5 have not yet been identified. Here we analyzed the impact of the deletion of *Pcgf5* specifically in hematopoietic stem and progenitor cells (HSPCs). *Pcgf5* is expressed preferentially in hematopoietic stem cells (HSCs) and multipotent progenitors (MPPs) compared with committed myeloid progenitors and differentiated cells. We transplanted bone marrow (BM) cells from *Rosa::Cre-ERT* control and *Cre-ERT;Pcgf5*$^{fl/fl}$ mice into lethally irradiated recipient mice. At 4 weeks post-transplantation, we deleted *Pcgf5* by injecting tamoxifen, however, no obvious changes in hematopoiesis was detected including the number of HSPCs during a long-term observation period following the deletion. Competitive BM repopulating assays revealed normal repopulating capacity of *Pcgf5*-deficient HSCs. Nevertheless, *Pcgf5*-deficient HSPCs showed a significant reduction in H2AK119ub1 levels compared with the control. ChIP-sequence analysis confirmed the reduction in H2AK119ub1 levels, but revealed no significant association of changes in H2AK119ub1 levels with gene expression levels. Our findings demonstrate that Pcgf5-containing PRC1 functions as a histone modifier *in vivo*, but its role in HSPCs is limited and can be compensated by other PRC1-related complexes in HSPCs.

Introduction

Epigenetic regulation has a critical role not only in normal hematopoiesis but also in hematological malignancies [1-3]. Polycomb-group (PcG) proteins are key regulators of the epigenetic machinery that establish and maintain reversible gene silencing. PcG proteins form various polycomb repressive complexes (PRC). The PRC1 and PRC2 complexes possess H2AK119 ubiquitin ligase activity and H3K27 methyltransferase activity, respectively. Six PRC1-related complexes containing distinct Polycomb-group RING finger proteins (Pcgf1-Pcgf6) have been identified [4,5].

PcG complexes have been well characterized as general regulators of stem cells [6,7]. Pcgf4/Bmi1, a component of canonical PRC1 (PRC1.4), plays a central role in the maintenance of self-renewal and multipotency of hematopoietic stem cells (HSCs) by targeting $p16^{Ink4a}$ and $p19^{Arf}$ tumor suppressor genes and developmental regulator genes [8-10]. PRC2 complex has a well-established role in the maintenance of HSCs [11,12]. In addition to their role in stem cells, PcG proteins also function in tumor-initiating cells, where they are often deregulated, leading to the promotion of tumorigenesis. Thus, PcG genes act as both oncogenes as well as tumor suppressor genes depending on cell type [3, 13-15].

PRC1.5 is one of the emerging variant PRC1 complexes, and consists of Ring1a/b, Pcgf5, Rybp/Yaf2 and Auts2. Pcgf5 and Auts2 are components unique to PRC1.5. Of interest, Auts2 has been shown to render PRC1 capable of activating transcription by recruiting casein kinase 2 and p300 in developing neuronal cells [16]. In contrast, Pcgf5 has been demonstrated to contribute to H2AK119ub1-dependent recruitment of PRC2 and H3K27me3 modification in a manner similar to other variant PRC1 complexes, Pcgf1 and Pcgf3, in a *de novo* targeting assay in mouse embryonic stem cells (ESCs) [17].

However, its role *in vivo* remains to be investigated.

In this study, we analyzed the role of Pcgf5 in hematopoietic stem and progenitor cells (HSPCs). Using a *Pcgf5* conditional knockout mouse model and comprehensive expression and epigenetic analyses, we demonstrate that Pcgf5 regulates global H2A monoubiquitylation but is dispensable for hematopoietic stem and progenitor cells.

Materials and Methods

Ethics Statement

Experiments using mice were performed in accordance with institutional guidelines of the Graduate School of Medicine, Chiba University. This study was approved by the Institutional Review Committees of Chiba University (approval numbers 24-64 and 27-213).

Mice and gene targeting of *Pcgf5*

The conditional *Pcgf5* allele (*Pcgf5*^{fl}), which contains LoxP sites flanking *Pcgf5* exon 2 containing the first ATG, was generated by homologous recombination using R1 embryonic stem (ES) cells according to the conventional protocol. *Pcgf5*$^{fl/+}$ mice were backcrossed to the C57BL/6 background more than 5 times and crossed with *Rosa::Cre-ERT2* mice (TaconicArtemis GmbH). To induce Cre activity, mice were injected with 100 μl of tamoxifen dissolved in corn oil at a concentration of 10 mg/ml intraperitoneally once a day for 5 consecutive days 1 month after transplantation. C57BL/6 mice congenic for the Ly5 locus (CD45.1) were purchased from Sankyo Lab Service.

Locus-specific genotyping of *Pcgf5*

We performed genotyping of *Pcgf5* allele using the following primers.

5’-GACCCTGAAGGAGTTGGCTCG-3’ and 5’- TGGCCTTGGTACACATATAGC-3’ for *flox* allele, and 5’-TGTTTACAGAGAGGAAGCGCC-3’ and 5’-TGGCCTTGGTACACATATAGC-3’ for *delta* allele.

Bone marrow transplantation

Bone marrow (BM) cells from test mice (CD45.2) were injected via the tail veins of 8-week-old CD45.1 recipients lethally irradiated at a dose of 9.5 Gy with or without competitor BM cells from 8-week-old CD45.1 congenic mice. For secondary transplantation, 5×10^6 BM cells pooled from the primary recipient mice at 4 months post-transplantation were injected into 8-week-old CD45.1 mice (secondary recipient mice) irradiated at a dose of 9.5 Gy without competitor cells.

Purification of hematopoietic cells and flow cytometric analysis

BM mononuclear cells were incubated with APC-conjugated anti-c-Kit antibody followed by anti-APC MicroBeads (Miltenyi Biotec). c-Kit$^+$ cells were immunomagnetically enriched by passing through an LS column (Miltenyi Biotec). Purified c-Kit$^+$ cells were then stained with a mixture of biotin-conjugated mAbs against lineage markers, including Gr-1, Mac-1, interleukin (IL)-7Rα, B220, CD4, CD8, and Ter119, and FITC-conjugated anti-CD34, PE-conjugated anti-FcγRII/III, PE-Cy7-conjugated anti-Sca-1, and APC-conjugated anti-c-Kit antibodies. Biotinylated antibodies were detected with APC-Cy7-conjugated streptavidin. CD45.1 and CD45.2 antibodies were used as additional markers for recipient cells and donor-derived cells, respectively. Flow cytometric analyses were performed using antibodies recognizing the following antigens: CD45.2 (104), CD45.1(A20), Gr-1 (RB6-8C5), CD11b/Mac-1 (M1/70), Ter-119, CD127/IL-7Rα (A7R34, SB/199), B220 (RA3-6B2), CD4 (GK1.5, RM4-5), CD8α (53–6.7), CD117/c-Kit (2B8), Sca-1 (D7), CD135 (A2F10) and CD16/32/FcγRII-III (93). The antibodies were purchased from BD Biosciences, eBioscience, and BioLegend. Dead cells were eliminated by staining with 0.5 μg/ml propidium iodide (Sigma-Aldrich). The data were acquired on a FACS Aria II cell sorter

or a Canto II flow cytometer (both BD Biosciences), and analyzed using Flowjo Version 10.0.6 software (TreeStar).

Chromatin immunoprecipitation (ChIP) assay and ChIP-Sequence analysis

FACS-sorted GMPs from the BM of recipient mice were cross-linked with 0.5% formaldehyde for 2 minutes at 37℃, washed twice with phosphate-buffered saline, suspended in ChIP buffer (10 mM Tris-HCl, pH 8.0, 200 mM NaCl, 1 mM $CaCl_2$, 0.5% NP-40, and protease inhibitor cocktail), sonicated 3 times for 5 seconds using Bioruptor (Cosmo Bio), digested by MNase (New England BioLabs) for 40 minutes at 37℃, lysed with radioimmunoprecipitation assay (RIPA) buffer (50mM Tris-HCl, pH 8.0, 150 mM NaCl, 2 mM EDTA, 1% NP-40, 0.1% SDS and 0.5% sodium deoxycholate) and then sonicated 10 times for 5 seconds using Bioruptor (Cosmo Bio). Dynabeads M-280 Sheep anti-Rabbit IgG (Life technologies) blocked with bovine serum albumin was used for collection of chromatin. Before the immunoprecipitation, 20 μl of Dynabeads was incubated with an anti–H3K27me3 antibody (07-449; Millipore) or an anti–monoubiquitinated H2A (H2Aub1; 8240S, Cell Signaling Technology) for 2 hours at 4℃. Chromatin was immunoprecipitated overnight at 4℃ with antibody-conjugated Dynabeads. The immunoprecipitates were washed extensively with the following combination of wash buffers: ChIP buffer, ChIP wash buffer (10 mM Tris-HCl, pH 8.0, 500 mM NaCl, 1 mM $CaCl_2$, 0.5% NP-40), and TE buffer (10 mM Tris-HCl, pH 8.0, and 1 mM EDTA). Bound chromatin and input DNA were placed in ChIP elution buffer (50 mM Tris-HCl, pH 8.0, 10 mM EDTA and 1% SDS) and reverse cross-linked. Immunoprecipitated DNA and input DNA were treated with RNase A (Sigma-Aldrich) and proteinase K (Roche), and purified with a QIAquick PCR purification kit (Qiagen).

Libraries for ChIP-sequene were generated using ThruPLEX DNA-seq Kit (Rubicon genomics).

RNA-sequence

Total RNA isolation was performed using an RNeasy plus Micro Kit (Qiagen) according to the manufacturer's instructions. cDNA was synthesized using a SMARTer Ultra Low Input RNA Kit for Sequencing (Clontech). cDNA libraries were generated with $6x10^3$ LSK cells and GMPs using a NEBNext Ultra DNA Library Prep Kit (New England BioLabs) according to the manufacturer's indications. The RNA-sequence reads were aligned using TopHat 1 (version 2.0.13; with default parameters) and levels of gene expression were quantified using Cufflinks (version 2.2.1).

RT-qPCR.

Total RNA was isolated using TRIZOL LS solution (Invitrogen) and reverse-transcribed by the ThermoScript RT-PCR system (Invitrogen) with an oligo-dT primer. Quantitative RT-PCR (RT-qPCR) was performed with a StepOnePlus Real-Time PCR System (Life Technologies) using FastStart Universal Probe Master (Roche) and the indicated combinations of Universal Probe Library (Roche) and primers listed below. *Hprt* expression was used to calculate relative expression levels. Probe numbers and primer sequences were: Probe #26, 5'-AGATGGCGACTAAGAG GAGAAA-3' and 5'-ACAAATAGTGCAGGATTCATTCAG-3' for *Pcgf5*; and probe #95, 5'-TCCTCCTCAGACCGCTTTT-3' and 5'- CCTGGTTCATCATCGCTAATC-3' for *Hprt*. To amplify truncated *Pcgf5* mRNA, primers directed to exon 1 and exon 5/6 junction were used: 5'-GGCGCTGTTTCTCTTTCGC-3' for exon 1 and 5'-

CTTCGAAATATCATCTTGCCC-3’ for exon 5/6 junction.

Immunoprecipitation and Western blot analysis for histone modification

Pcgf5$^{fl/fl}$*;Rosa::Cre-ERT2* ES cells were derived from blastocysts. Conditional deletion of *Pcgf5* was carried out by the addition of 800 nM 4-hydroxytamoxifen for 48 h in culture. For collection, ES cells were trypsinized and plated to gelatin-coated dishes for 30 min to remove contaminating feeder cells. The cells were lysed in 0.1% NP-40 lysis buffer (300 mM NaCl) and centrifuged. The resulting supernatants were kept on ice (Solution A). The pellets were resuspended in 0.1% NP-40 lysis buffer (300 mM NaCl) and sonicated using a Bioruptor (Cosmo Bio) (Solution B). The mixtures of Solution A and Solution B were diluted with 0.1% NP-40 lysis buffer (0 mM NaCl) until the final NaCl concentrations reached 150 mM. After centrifugation, the resulting supernatants were used as input lysates for immunoprecipitation, which was performed using an anti-Ring1b antibody (D139-3, MBL). Total lysates were used to detect histone proteins. Proteins were separated by SDS-PAGE, transferred to a PVDF membrane and detected by Western blotting using the following antibodies: anti-Pcgf5 antibody (ab76724, Abcam), anti-H3 (ab1791, Abcam), anti-H3K27me3 (07-449, Millipore), anti-H2A (ab18255, Abcam), and anti-H2AK119ub (8240S, Cell Signaling Technology). The protein bands were detected with enhanced chemiluminescence reagent (Immobilon Western, Millipore). Sequential reprobing of membranes with antibodies was performed after the removal of primary and secondary antibodies from membranes in 0.2M glycine-HCl buffer (pH 2.5) and/or inactivation of HRP by 0.1% NaN3.

Statistical analysis

Statistical tests were carried out using Graph Pad Prism version 6. Data are shown as the mean ± SD. Statistical significance was taken at values of *p less than .05, ** p less than .01, and *** p less than .001.

Accession numbers

RNA-sequence and ChIP-sequence data were deposited in DNA Data Bank of Japan (DDBJ) (accession number DRA004231).

Results

Pcgf5 is preferentially expressed in hematopoietic stem and progenitor cells

We first analyzed the expression of *Pcgf5* in hematopoietic cells by RT-PCR. *Pcgf5* appeared to be preferentially expressed in CD34$^-$ Flt3$^-$ Lineage marker$^-$ Sca-1$^+$ c-Kit$^+$ (CD34$^-$LSK) long-term (LT)-HSCs, CD34$^+$Flt3$^-$LSK short-term (ST)-HSCs and CD34$^+$Flt3$^+$LSK multipotent progenitor cells (MPPs), but downregulated during differentiation (Fig 1A). To understand the role of Pcgf5 in hematopoietic stem and progenitor cells (HSPCs), we generated mice harboring *Pcgf5^{fl}* allele in which exon 2 containing the first ATG is floxed (Fig 1B) and then crossed *Pcgf5$^{fl/fl}$* mice with *Rosa26::Cre-ERT (Cre-ERT) mice* to generate *Cre-ERT;Pcgf5$^{fl/fl}$ mice*.

To exclude any influences of the loss of *Pcgf5* on organs other than hematopoietic system, we transplanted BM cells from *Cre-ERT* control and *Cre-ERT;Pcgf5$^{fl/fl}$* mice with and without competitor cells into lethally irradiated recipient mice (CD45.1) and deleted *Pcgf5* by intraperitoneal injection of tamoxifen at 1 month post-transplantation (Fig 1C). We confirmed the efficient deletion of *Pcgf5* by genomic PCR of CD45.2 donor cells in the PB (Fig 1D). We also confirmed the generation of a short form of *Pcgf5* mRNA lacking exon 2 in BM Lineage marker$^-$ c-Kit$^+$ (LK) progenitor cells after injection of tamoxifen (Fig 1E). Pcgf5 functions as a component of PRC1.5. In order to examine whether the functional Pcgf5 proteins are translated from the internal ATG of the short form of *Pcgf5* mRNA, we prepared lysates from *Pcgf5$^{fl/fl}$* and *Pcgf5$^{\Delta/\Delta}$* ES cells, and immunoprecipitated Ring1b. Pcgf5 was readily detected in the immunoprecipitates from *Pcgf5$^{fl/fl}$* cells, but not *Pcgf5$^{\Delta/\Delta}$* cells. Even the short form of Pcgf5 was not detected in immunoprecipitates from *Pcgf5$^{\Delta/\Delta}$* ES cells. These results indicate that no functional Pcgf5 protein that can bind Ring1b is translated from the truncated *Pcgf5* mRNA lacking

the first ATG (Fig 1F). The level of Ring1b protein did not largely change in *Pcgf5*$^{\Delta/\Delta}$ hematopoietic cells and ES cells (data not shown).

Deletion of *Pcgf5* in adult hematopoietic cells does not compromise hematopoiesis

In order to evaluate the role of Pcgf5 in HSPCs, we first transplanted BM cells from *Cre-ERT* control and *Cre-ERT;Pcgf5*$^{fl/fl}$ mice without competitor cells into lethally irradiated recipient mice. After the deletion of *Pcgf5*, PB cell counts showed moderate reduction in white blood cell (WBC) counts in *Pcgf5*$^{\Delta/\Delta}$ mice, although it did not reach statistical significant levels (Fig 2A). RBC counts, hemoglobin content and platelet counts did not significantly change in the absence of Pcgf5 (Fig 2A). In addition, no obvious change of lineage contribution of donor cells to PB hematopoietic cells was detected after the deletion of *Pcgf5* (Fig 2B). Correspondingly, BM analysis at 4 months post-deletion of *Pcgf5* revealed no significant changes in the number of total BM cells (Fig 2C), LSK HSPCs, common lymphoid progenitors (CLPs) and myeloid progenitors including common myeloid progenitors (CMPs), granulocyte-macrophage progenitors (GMPs), and megakaryocyte-erythroid progenitors (MEPs) (Fig 2D).

We next explored the consequences of *Pcgf5* loss on the competitive repopulating capacity of HSPCs. We transplanted BM cells from *Cre-ERT* control and *Cre-ERT;Pcgf5*$^{fl/fl}$ mice with the same number of competitor cells from CD45.1 congenic wild-type (WT) mice into lethally irradiated recipient mice. Even in this competitive setting, no evident changes were detected in chimerism of CD45.2^{+} *Pcgf5*$^{\Delta/\Delta}$ cells in the PB compared with the control (Fig 3A). BM analysis at 3 months post-deletion of *Pcgf5* revealed a mild but significant increase in the chimerism of CD45.2^{+} *Pcgf5*$^{\Delta/\Delta}$ cells in total cells, LSK HSPCs, CLPs, and myeloid progenitors in the BM (Fig 3B), but not in splenic

LSK cells nor total thymocytes in the thymus (Fig 3C). To further evaluate the repopulating capacity of *Pcgf5*$^{\Delta/\Delta}$ HSPCs, we analyzed BM from secondary recipients transplanted with pooled BM cells from primary mice. Chimerism of *Pcgf5*$^{\Delta/\Delta}$ cells was comparable to WT cells in both PB and BM of secondary recipients (Figs 3D and E). The trend of *Pcgf5*$^{\Delta/\Delta}$ HSPCs toward higher chimerism in the BM of primary mice totally disappeared in the secondary recipients. These results suggest that the loss of *Pcgf5* does not significantly alter reconstitution capacity of HSPCs.

Loss of Pcgf5 has a limited effect on the transcriptional profiles of HSPCs

To understand the effects of Pcgf5 loss on HSPCs, we next purified LSK HSPCs and GMPs from BM at 4 months post-deletion of *Pcgf5* and performed RNA-sequence analysis. RNA-sequence data confirmed the absence of *Pcgf5* transcript corresponding to exon 2 deleted in *Pcgf5*$^{\Delta/\Delta}$ cells (Fig 4A). The number of genes altered greater than 2-fold in the absence of Pcgf5 was relatively small (Fig 4B) and the expression changes were mild (Fig 4B). Indeed, the levels of expression changes in *Pcgf5*$^{\Delta/\Delta}$ cells were not statistically significant compared with WT cells (Fig 4C). Genes upregulated greater that 2-fold in *Pcgf5*$^{\Delta/\Delta}$ LSK cells significantly overlapped with those in *Ezh2*$^{\Delta/\Delta}$ LSK cells [18], but, of interest, barely with those in *Pcgf4/Bmi1*$^{\Delta/\Delta}$ LSK cells [19] (Fig 4D). Given the minimal hematological phenotypes in the absence of Pcgf5, we assumed that the other Pcgf family genes were activated to complement Pcgf5 loss. However, RNA-seq data did not show activation of any other family genes in the absence of Pcgf5 (Fig 4E). Nevertheless, RNA-sequence data revealed that the expression of *Pcgf1* and *Pcgf5* in Reads Per Kilobase of exon per Million mapped fragments (RPKM) was much higher than the other member genes in LSK cells and GMPs (Fig 4E), suggesting that *Pcgf1* and

Pcgf5 are the major Pcgf family genes expressed in HSPCs.

Global levels of H2AK119ub1 are significantly reduced in the absence of Pcgf5

As shown in Figure 1F, Pcgf5 functions as a component of PRC1-related complex. As expected from these data, global H2AK119ub1 level was decreased by 40% in *Pcgf5*$^{\Delta/\Delta}$ Lin^{-}c-Kit^{+} progenitor cells in Western blot analysis, while H3K27 level was not altered in the absence of Pcgf5 (Fig 5A).

We next performed ChIP-sequence analysis of H2AK119ub1 and H3K27me3 in GMPs from recipient mice at 4 months post-deletion of *Pcgf5*. We defined genes with ≥ 2-fold enrichment of H2AK119ub1 ChIP signals over the input signals at the promoter region (2.0 kb ± transcriptional start sites) as H2AK119ub1 genes (Fig 5B). H2AK119ub1 genes in WT GMPs significantly overlapped with genes marked with H2AK119ub1 in ES cells [20] (Fig 5C). Importantly, nearly 20 % of H2AK119ub1 genes showed reduction in H2AK119ub1 levels ≥ 2-fold upon loss of Pcgf5 in GMPs (Figs 5B and C). Indeed, H2AK119ub1 ChIP signals over the input signals were significantly reduced in *Pcgf5*$^{\Delta/\Delta}$ GMPs compared with WT GMPs, while those of H3K27me3 showed a very mild albeit significant increase in *Pcgf5*$^{\Delta/\Delta}$ GMPs (Figs 5D). Polycomb-related histone marks, H2AK119ub1 and H3K27me3, mutually reinforce each other and behave in a similar manner in many settings. Unexpectedly, however, H2AK119ub1 genes that showed reduction in H2AK119ub1 levels ≥ 2-fold in *Pcgf5*$^{\Delta/\Delta}$ GMPs (*Pcgf5*$^{\Delta/\Delta}$_Down genes) showed a significant increase in H3K27me3 levels (Fig 5D). In contrast to our expectation, comparison of ChIP signals with expression changes revealed no significant correlation of reduced H2AK119ub1 levels with gene expression (Figs 5E and F). Moreover, *Pcgf5*$^{\Delta/\Delta}$*_D*own genes (listed in gene symbol) little overlapped with genes upregulated

greater than 2-fold in *Pcgf5*$^{\Delta/\Delta}$ GMPs relative to WT GMPs (*Pcgf5*$^{\Delta/\Delta}$ GMPs_Exp_Up)(Figure 5G). These findings well correspond to the mild changes in global gene expression and minimal hematological phenotypes in *Pcgf5*$^{\Delta/\Delta}$ HSPCs.

In order to understand the minimal effect of the loss of Pcgf5 in gene expression, we overexpressed 3xFlag-Pcgf1 and 3xFlag-Pcgf5 in mouse erythroleukemia (MEL) cells and performed ChIP-sequence analysis of Pcgf1, Pcgf5 and H2K119ub1. We found that Pcgf1 regulates more gene promoters (2.0 kb ± transcriptional start sites) than Pcgf5 and also bound most of the Pcgf5 targets (82.1%). Among Pcgf5 targets, Pcgf1 regulated the majority of Pcgf5 targets associated with the H2AK119ub1 modification (89.3%) in MEL cells. (Fig 5H and Table 1). These findings suggest that Pcgf1 largely compensates for the loss of Pcgf5.

Discussion

In this study, we generated *Pcgf5* conditional knockout mice and found that the hematopoietic-specific deletion of *Pcgf5* results in no significant changes in hematopoiesis compared with control mice. However, Pcgf5 appeared to contribute to the global monoubiqutination of H2AK119 in hematopoietic cells. Although the absence of Pcgf5 did not greatly affect the gene expression profiles of HSPCs, our findings provide the first direct evidence that supports PRC1-related function of Pcgf5 that is involved in the regulation of H2AK119ub1.

Pcgf5 has repeatedly been identified as a component of variant PRC1 that include Auts2 (PRC1.5). As other Pcgf family proteins, Pcgf5 has been thought to support the monoubiquitination of H2AK119 by Ring1b, however, this has never been conformed *in vivo*. In this study, *Pcgf5*-deficient HSPCs clearly showed reduction in H2AK119ub1 levels. Nearly 20 % of gene promoters (1,147 genes) marked with H2AK119ub1 in WT GMPs reduced H2AK119ub1 levels greater that 2-fold in GMPs in the absence of Pcgf5. This finding suggests that Pcgf5 targets a large number of genes and plays a major role in the regulation of H2AK119ub1. Upregulated genes in *Pcgf5*-deficient LSK cells significantly overlapped with those in *Ezh2*-deficient LSK cells, suggesting that Pcgf5 targets largely overlap with those of PRC2. In contrast, however, upregulated genes in *Pcgf5*-deficient LSK cells did not significantly overlap with those in *Pcgf4/Bmi1*-deficient LSK cells, suggesting that Pcgf5 in variant PRC1 regulates genes distinct from those of canonical PRC1 that contains Pcgf4/Bmi1 in HSPCs. Recently, Pcgf2/Mel18-containing PRC1 complexes have been reported to exchange subunits in a stage-specific manner during cardiac differentiation and regulate both transcriptional repression and activation of distinctive sets of target genes [21]. Because more genes were

downregulated upon *Pcgf5* deletion, Pcgf5 could function like Pcgf2/Mel18 in a context-specific manner.

As described above, Pcgf5 as well as Pcgf1 and Pcgf3, has been shown to recruit PRC2 in an H2AK119ub1-dependent manner and induce H3K27me3 modification at its target genes in a *de novo* targeting assay in mouse ESCs [17]. Therefore, we expected to see a reduction in H3K27me3 levels at the Pcgf5 target genes. However, H2AK119ub1 genes that showed reduction in H2AK119ub1 levels (≥ 2-fold) in *Pcgf5*$^{\Delta/\Delta}$ GMPs (*Pcgf5*$^{\Delta/\Delta}$_Down genes) displayed rather increased H3K27me3 levels at their promoters. Although the molecular mechanism underlying this epigenomic alteration remains unclear, it is possible that several different pathways that recruit polycomb complexes exist as backup, and some of them could be activated in a setting of polycomb dysfunction. In the case of Pcgf5 loss, we identified augmentation in H3K27me3 levels, which might represent activation of the compensatory pathway and could be responsible for the maintenance of transcriptional repression of the *Pcgf5*$^{\Delta/\Delta}$_down genes in HSPCs.

Pcgf5 expression is high in HSPCs compared with differentiated cells and appeared to be the major Pcgf family gene expressed in HSPCs. RNA-sequence data demonstrated that *Pcgf1* and *Pcgf5* are most abundant in HSPCs. However, the impact of loss of Pcgf5 was very limited in HSPCs. These findings suggest that Pcgf5 function could be compensated by other family members such as Pcgf1, which is highly expressed in HSPCs. Pcgf1 is the component of the non-canonical PRC1 complex, PRC1.1, and has been demonstrated to cause a drastic reduction in H2AK119ub1 levels in murine ESCs upon knockdown [22]. Indeed, ChIP-sequence analysis in MEL cells demonstrated that Pcgf5 targets are mostly co-regulated by Pcgf1. Given that the loss of Pcgf5 was largely compensated for in HSPCs, the role of Pcgf1-containing PRC1.1 could be more critical

than Pcgf5-containing PRC1.5 in the maintenance of HSPCs. Further study of non-canonical PRC1 complexes is needed to decipher their physiological functions in HSPCs.

Although Pcgf5 appears to be dispensable for hematopoiesis, Pcgf family gene expression could vary in different organs and tissues and Pcgf5 may be required for the proliferation, survival and function of certain types of cells. The mice that harbor floxed allele for *Pcgf5* generated in this study should serve as a valuable tool to analyze the role of Pcgf5 in those cells.

Acknowledgements

My deepest gratitude goes first and foremost to Professor Atsushi Iwama, my supervisor, for his constant encouragement and guidance.

Second, I would like to express my heartfelt gratitude to Dr. Yaeko Nakajima-Takagi, who has instructed and helped me a lot throughout my study.

Last my thanks would go to Kazumasa Aoyama, Motohiko Oshima, Atsunori Saraya, Hiroki Sugishita, Manabu Nakayama, Tomoyuki Ishikura and Haruhiko Koseki for research assistance. I also owe my sincere gratitude to Changshan Wang and Shuhei Koide for technical assistance and Ola Mohammed Kamel Rizq for critical review of the manuscript.

References

1. Oshima, M., and Iwama A. (2014) Epigenetics of hematopoietic stem cell aging and disease. *Int J Hematol* **100,** 326-334.
2. Beerman I, Rossi DJ. (2015) Epigenetic Control of Stem Cell Potential during Homeostasis, Aging, and Disease. *Cell Stem Cell* **16**, 613-625.
3. Shih AH, Abdel-Wahab O, Patel JP, and Levine RL. (2012) The role of mutations in epigenetic regulators in myeloid malignancies. *Nat Rev Cancer* **12,** 599-612.
4. Gao Z, Zhang J, Bonasio R, Strino F, Sawai A, Parisi F, Kluger Y, Reinberg D. (2012) PCGF homologs, CBX proteins, and RYBP define functionally distinct PRC1 family complexes. *Mol Cell* **45,** 344-356.
5. Comet I, Helin K. (2014) Revolution in the Polycomb hierarchy. *Nat Struct Mol Biol* **21,** 573-575.
6. Sauvageau M, Sauvageau G. (2010) Polycomb group proteins: multi-faceted regulators of somatic stem cells and cancer. *Cell Stem Cell* **7,** 299-313.
7. Laugesen A, Helin K. (2014) Chromatin repressive complexes in stem cells, development, and cancer. *Cell Stem Cell* **14,** 735-751.
8. Park IK, Qian D, Kiel M, Becker MW, Pihalja M, Weissman IL, Morrison SJ, Clarke MF. (2003) Bmi-1 is required for maintenance of adult self-renewing haematopoietic stem cells. *Nature* **423**, 302-305.
9. Oguro H, Iwama A, Morita Y, Kamijo T, van Lohuizen M, Nakauchi H. (2006) Differential impact of Ink4a and Arf on hematopoietic stem cells and their bone marrow microenvironment in Bmi1-deficient mice. *J Exp Med* **203,** 2247-2253.

10. Oguro H, Yuan J, Ichikawa H, Ikawa T, Yamazaki S, Kawamoto H, Nakauchi H, Iwama A. (2010) Poised lineage specification in multipotential hematopoietic stem and progenitor cells by the polycomb protein Bmi1. *Cell Stem Cell* **6,** 279-286.

11. Xie H, Xu J, Hsu JH, Nguyen M, Fujiwara Y, Peng C, Orkin SH. (2014) Polycomb repressive complex 2 regulates normal hematopoietic stem cell function in a developmental-stage-specific manner. *Cell Stem Cell* **14,** 68-80.

12. Hidalgo I, Herrera-Merchan A, Ligos JM, Carramolino L, Nuñez J, Martinez F, Dominguez O, Torres M, Gonzalez S.(2012) Ezh1 is required for hematopoietic stem cell maintenance and prevents senescence-like cell cycle arrest. *Cell Stem Cell* **11,** 649-662

13. Morin RD, Johnson NA, Severson TM, Mungall AJ, An J, Goya R, Paul JE, Boyle M, Woolcock BW, Kuchenbauer F, Yap D, Humphries RK, Griffith OL, Shah S, Zhu H, Kimbara M, Shashkin P, Charlot JF, Tcherpakov M, Corbett R, Tam A, Varhol R, Smailus D, Moksa M, Zhao Y, Delaney A, Qian H, Birol I, Schein J, Moore R, Holt R, Horsman DE, Connors JM, Jones S, Aparicio S, Hirst M, Gascoyne RD, Marra MA. (2010) Somatic mutations altering EZH2 (Tyr641) in follicular and diffuse large B-cell lymphomas of germinal-center origin. *Nat Genet* **42,** 181–185.

14. Ernst T, Chase AJ, Score J, Hidalgo-Curtis CE, Bryant C, Jones AV, Waghorn K, Zoi K, Ross FM, Reiter A, Hochhaus A, Drexler HG, Duncombe A, Cervantes F, Oscier D, Boultwood J, Grand FH, and Cross NC. (2010) Inactivating mutations of the histone methyltransferase gene EZH2 in myeloid disorders. *Nat Genet* **42,** 722–726.

15. Nikoloski G, Langemeijer SM, Kuiper RP, Knops R, Massop M, Tönnissen ER, van der Heijden A, Scheele TN, Vandenberghe P, de Witte T, van der Reijden BA, Jansen

JH. (2010) Somatic mutations of the histone methyltransferase gene EZH2 in myelodysplastic syndromes. *Nat Genet* 42, 665–667.

16. Gao Z, Lee P, Stafford JM, von Schimmelmann M, Schaefer A, Reinberg D. (2014) AUTS2-Polycomb complex activates gene expression in the CNS. *Nature* **516,** 349-354.

17. Blackledge NP, Farcas AM, Kondo T, King HW, McGouran JF, Hanssen LL, Ito S, Cooper S, Kondo K, Koseki Y, Ishikura T, Long HK, Sheahan TW, Brockdorff N, Kessler BM, Koseki H, Klose RJ. (2014) Variant PRC1 complex-dependent H2A ubiquitylation drives PRC2 recruitment and polycomb domain formation. *Cell* **157,** 1445-1459.

18. Mochizuki-Kashio M, Aoyama K, Sashida G, Oshima M, Tomioka T, Muto T, Wang C, Iwama A. (2015) Ezh2 loss in hematopoietic stem cells predisposes mice to develop heterogeneous malignancies in an Ezh1-dependent manner. *Blood* **126,** 1172-1183.

19. Oguro H, Yuan J, Ichikawa H, Ikawa T, Yamazaki S, Kawamoto H, Nakauchi H, and Iwama A. (2010) Poised lineage specification in multipotent hematopoietic stem and progenitor cells by the polycomb protein Bmi1. *Cell Stem Cell* **6,** 279-286.

20. Morey L, Aloia L, Cozzuto L, Benitah SA, Di Croce L. (2013) RYBP and Cbx7 define specific biological functions of polycomb complexes in mouse embryonic stem cells. *Cell Rep* **3**, 60-69.

21. Morey L, Santanach A, Blanco E, Aloia L, Nora EP, Bruneau BG, Di Croce L. (2015) Polycomb Regulates Mesoderm Cell Fate-Specification in Embryonic Stem Cells through Activation and Repression Mechanisms. *Cell Stem Cell* **17,** 300-315.

22. Wu X, Johansen JV, Helin K. (2013) Fbxl10/Kdm2b recruits polycomb repressive complex 1 to CpG islands and regulates H2A ubiquitylation. *Mol Cell* **49,** 1134-1146.

Figure legends

Figure 1. Generation of conditional knockout allele for *Pcgf5* in mice

(A) RT-PCR analysis of *Pcgf5* in BM hematopoietic cell fractions. Cells analyzed were $CD34^-$LSK long-term HSCs, $CD34^+Flt3^-$LSK short-term HSCs, $CD34^+Flt3^+$LSK multipotent progenitors (MPPs), common myeloid progenitors (CMPs), granulocyte-macrophage progenitors (GMPs), megakaryocyte-erythroid progenitors (MEPs), and lineage marker$^+$ mature hematopoietic cells. *Hypoxanthine-guanosine phosphoribosyl transferase (Hprt)* was used as a housekeeping control gene. Data are shown as the mean ± standard deviation (SD) for triplicate analyses. (B) Strategy for making a conditional knockout allele for *Pcgf5* by homologous recombination in ES cells. FRT recombinase was used to remove the *Neo* cassette. (C) Scheme of the hematopoietic repopulation assay. Total BM cells ($5x10^6$ cells) from *Cre-ERT* and *Cre-ERT;Pcgf5$^{fl/fl}$* were transplanted into lethally irradiated CD45.1 recipient mice without competitor BM cells, or $2x10^6$ total BM cells were transplanted with the same number of competitor BM cells. To induce deletion of *Pcgf5*, 100 μl of tamoxifen (10 mg/ml) was intraperitoneally injected once a day for five consecutive days at 1 month post-transplantation. (D) Efficient deletion of *Pcgf5* in hematopoietic cells detected by genomic PCR. Deletion of *Pcgf5* in *Cre-ERT;Pcgf5$^{fl/fl}$* PB myeloid cells was evaluated pre- and post-tamoxifen treatment. "WT", "Floxed", and "*Δ*" alleles indicate the wild-type and floxed *Pcgf5* allele, and floxed *Pcgf5* allele after removal of exon 2 by Cre recombinase, respectively. (E) Detection of truncated *Pcgf5* mRNA in BM *Pcgf5$^{Δ/Δ}$* LK cells using primers directed to exons 1 and exon 5/6 junction. (F) Pcgf5 interacts with Ring1B. Ring1B in lysates from *Pcgf5$^{fl/fl}$* and *Pcgf5$^{Δ/Δ}$* ES cells was immunoprecipitated using anti-Ring1b antibody,

and then immunoprecipitates were detected by immunoblotting using anti-Ring1b and anti-Pcgf5 antibodies.

Figure 2. Depletion of *Pcgf5* does not compromise adult hematopoiesis

(A) PB cell counts of recipients repopulated with *Cre-ERT* (+/+) and *Cre-ERT;Pcgf5*$^{fl/fl}$ BM cells after deletion of *Pcgf5* (*Δ/Δ*) by tamoxifen injection. Data are shown as mean ± SD (n=4-5). (B) Lineage contribution of donor cells to myeloid (Gr-1$^+$ and/or Mac-1$^+$), B (B220$^+$), or T (CD4$^+$ and/or CD8$^+$) cells in the PB shown as mean ± SD (n=4-5). (C) Absolute number of CD45.2$^+$ donor-derived hematopoietic cells in a unilateral pair of femur and tibia of recipients at 5 months post-transplantation. Data are shown as mean ± SD (WT, n=5; *Pcgf5*$^{Δ/Δ}$, n=6). (D) Absolute number of CD45.2$^+$ donor-derived LSK cells, CLPs and myeloid progenitors in the BM of recipient mice at 5 months post-transplantation presented as mean ± SD (WT, n=5; *Pcgf5*$^{Δ/Δ}$, n=6). n.s., not significant.

Figure 3. *Pcgf5*-deficient HSPCs retain normal reconstitution capacity of hematopoiesis

(A) Chimerism of donor-derived cells in recipients in competitive reconstitution assays using the same number of test cells (*Cre-ERT* and *Cre-ERT;Pcgf5*$^{fl/fl}$) and competitor cells. After engraftment, *Pcgf5* was deleted (*Pcgf5*$^{Δ/Δ}$) by tamoxifen injection. Data are shown as mean ± SD (n=4-5). (B) Chimerism of donor-derived CD45.2$^+$ hematopoietic cells in total BM cells, LSK cells, CLPs and myeloid progenitor fractions at 4 months post-transplantation. The data are shown as mean ± SD (n=7). (C) Chimerism of donor-derived CD45.2$^+$ cells in splenic LSK cells and donor-derived CD45.2$^+$ thymocytes in the thymus at 4 months post-transplantation shown as mean ± SD (n=3). (D, E) Secondary

transplantation assays. Total BM cells ($5x10^6$) from primary recipient mice at 4 months post-transplantation were transplanted into lethally irradiated secondary recipient mice without competitor cells. Chimerism of donor-derived cells in the PB (D) and total $CD45.2^+$ hematopoietic cells and LSK cells in the BM (E) at 5 months post-transplantation are shown as mean ± SD (WT, n=4; *Pcgf5*$^{\Delta/\Delta}$, n=5). *p<0.05; n.s., not significant.

Figure 4. Gene expression profile of *Pcgf5*-deficient HSPCs

(A) Snapshots of RNA-sequence signals at the *Pcgf5* gene locus in WT and *Pcgf5*$^{\Delta/\Delta}$ LSK cells isolated from recipient mice repopulated with *Pcgf5*$^{\Delta/\Delta}$ hematopoietic cells. The structure of *Pcgf5* gene locus including relevant exons is indicated at the bottom. (B) Scatter diagrams showing RNA-sequence data of LSK cells and GMPs. Expression levels of RefSeq genes (listed in RefSeq ID) defined by reads per kilobase of exon per million fragments mapped (RPKM) in log2 in WT and *Pcgf5*$^{\Delta/\Delta}$ cells are plotted. The light gray lines represent the boundaries for twofold increase and twofold decrease, respectively. The number of genes upregulated and downregulated more than twofold in *Pcgf5*$^{\Delta/\Delta}$ cells compared with WT cells are indicated in red and blue, respectively. (C) Box-and-whisker plots showing the expression levels of WT and *Pcgf5*$^{\Delta/\Delta}$ LSK cells and GMPs in RPKM. Boxes represent 25-75 percentile ranges. Vertical lines represent 10-90 percentile ranges. Horizontal bars represent medians. n.s., not significant. (D) Venn diagram showing the overlap between genes (listed in gene symbol) up-regulated in LSK cells from *Pcgf5*$^{\Delta/\Delta}$, *Ezh2*$^{\Delta/\Delta}$ [18], and *Bmi1* KO [19] mice (≥2.0-fold compared with the WT control, respectively). The numbers of genes in each group are indicated. The statistical

significance of the overlaps between the two gene groups is indicated. (E) Expression of *Pcgf* genes in WT LSK cells and GMPs in RPKM.

Figure 5. Loss of Pcgf5 results in reduction in global H2AK119 levels

(A) H2AK119ub1 levels in LK cells. LK cells from BM of WT and *Pcgf5*$^{\Delta/\Delta}$ mice were analyzed by Western blotting using anti-H2AK119ub1 and anti-H3K27me3 antibodies at 1-month post deletion of *Pcgf5*. Levels of H2AK119ub1 and H3K27me3 were normalized to the amount of H2A and H3, respectively, and are indicated relative to wild-type control values at the bottom. The representative data from two independent experiments are presented. (B) Scatter plots showing the correlation of the fold enrichment values against the input signals (ChIP/input) (transcription start site ±2.0 kb) of H2AK119ub1 and H3K27me3 of RefSeq genes (listed in RefSeq ID) between *WT* and *Pcgf5*$^{\Delta/\Delta}$ GMPs. The light gray lines represent the boundaries for twofold increase and twofold decrease, respectively. The changes of H2AK119ub1 or H3K27me3 levels in genes upregulated and downregulated more than twofold in *Pcgf5*$^{\Delta/\Delta}$ cells compared with WT cells are indicated in blue and red, respectively. (C) Venn diagram showing the overlap between H2AK119ub1 genes (listed in gene symbol) in GMPs and ES cells. *Pcgf5*$^{\Delta/\Delta}$ *_D*own genes are also depicted. (D) Box-and-whisker plots showing H2AK119ub1 and H3K27me3 levels in all Refseq genes (All genes) and H2AK119ub1 genes (genes with ≥ 2-fold enrichment of H2AK119ub1 ChIP signals over the input signals at 2.0 kb ± TSSs in WT GMPs) which showed reduction in H2AK119ub1 levels ≥ 2-fold in *Pcgf5*$^{\Delta/\Delta}$ GMPs (*Pcgf5*$^{\Delta/\Delta}$*_D*own genes). ***p <0.001 (Student t test). (E) Scatter plots showing the correlation of the fold expression and fold enrichment of H2AK119ub1 ChIP signals in *Pcgf5*$^{\Delta/\Delta}$ GMPs compared with those in WT GMPs. The

genes showing reduction in H2AK119ub1 levels greater than 2-fold (below dotted line) are indicated in red dots. The score of correlation coefficient between the fold expression and fold enrichment of H2AK119ub1 ChIP signals defined with Pearson's correlation and the linear regression are shown. (F) Box-and-whisker plots showing the expression levels of all RefSeq genes, H2AK119ub1 genes, and *Pcgf5*$^{\Delta/\Delta}$*_D*own genes in WT and *Pcgf5*$^{\Delta/\Delta}$ GMPs in RPKM. Boxes represent 25-75 percentile ranges. Vertical lines represent 10-90 percentile ranges. Horizontal bars represent medians. n.s., not significant. (G) Venn diagram showing the overlap between *Pcgf5*$^{\Delta/\Delta}$*_D*own genes (listed in gene symbol) in GMPs and genes upregulated in expression greater than 2-fold in *Pcgf5*$^{\Delta/\Delta}$ GMPs relative to WT GMPs. (H) ChIP-sequence data of 3xFlag-Pcgf1, 3xFlag-Pcgf5, and H2AK119ub1 in MEL cells. Venn diagram shows the overlap between Pcgf1 targets, Pcgf5 targets, and H2AK119ub1 genes (≥ 2-fold enrichment of ChIP signals over the input signals at 2.0 kb ± TSSs) (listed in gene symbol) in MEL cells.

Table 1. Target genes of Pcgf5, Pcgf1 and H2AK119ub1 in MEL cells identified by ChIP-Seq. (A). 441 common target genes of Pcgf5 and Pcgf1 with H2AK119ub1 modification. (B). 53 Pcgf5 target genes with H2AK119ub1 modification, but not bound by Pcgf1.

Figure 1

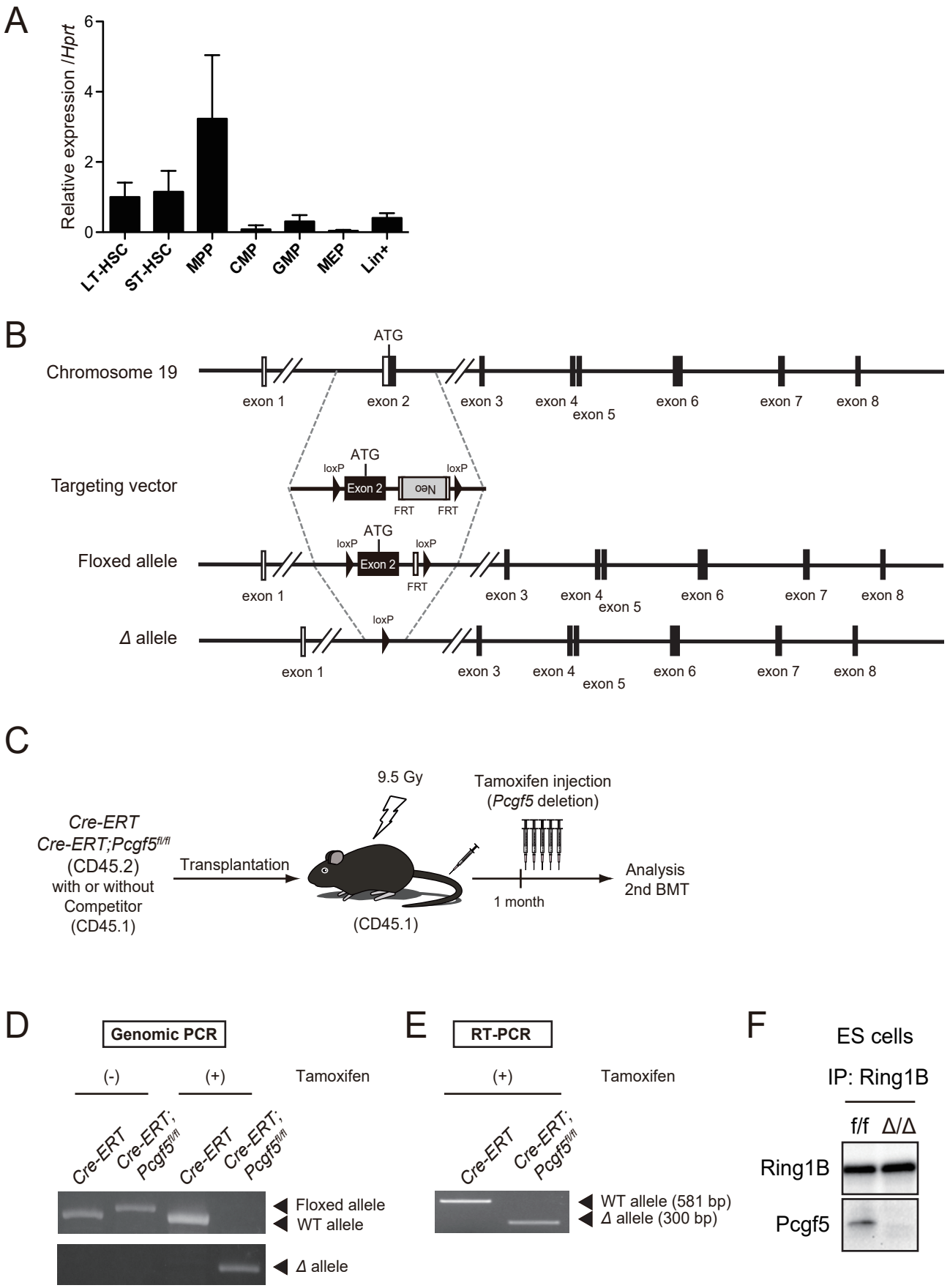
A
Relative expression /Hprt
6
4
2
0
LT-HSC
ST-HSC
MPP
CMP
GMP
MEP
Lin+
B
Chromosome 19
ATG
exon 1
exon 2
exon 3
exon 4
exon 5
exon 6
exon 7
exon 8
Targeting vector
loxP
Exon 2
Neo
FRT
Floxed allele
Δ allele
C
Cre-ERT
Cre-ERT;Pcgf5fl/fl
(CD45.2)
with or without
Competitor
(CD45.1)
Transplantation
9.5 Gy
Tamoxifen injection
(Pcgf5 deletion)
1 month
Analysis
2nd BMT
(CD45.1)
D
Genomic PCR
(-)
(+)
Tamoxifen
Cre-ERT
Cre-ERT; Pcgf5fl/fl
Floxed allele
WT allele
Δ allele
E
RT-PCR
WT allele (581 bp)
Δ allele (300 bp)
F
ES cells
IP: Ring1B
f/f
Δ/Δ
Ring1B
Pcgf5

Figure 2

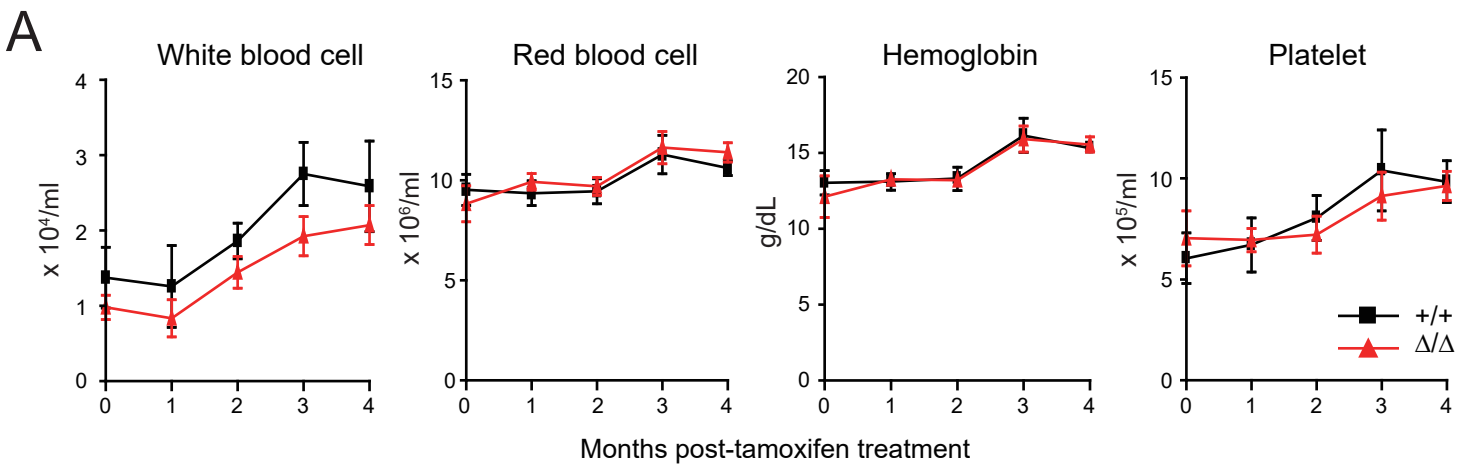
A
White blood cell
Red blood cell
Hemoglobin
Platelet
x 10⁴/ml
x 10⁶/ml
g/dL
x 10⁵/ml
+/+
Δ/Δ
Months post-tamoxifen treatment

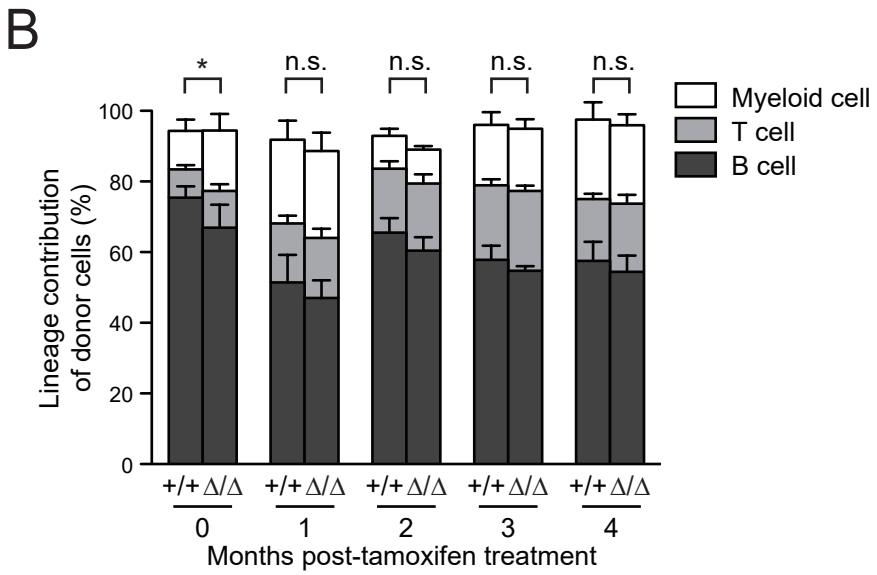
B
*
n.s.
n.s.
n.s.
n.s.
Myeloid cell
T cell
B cell
Lineage contribution of donor cells (%)
+/+ Δ/Δ
0
1
2
3
4
Months post-tamoxifen treatment

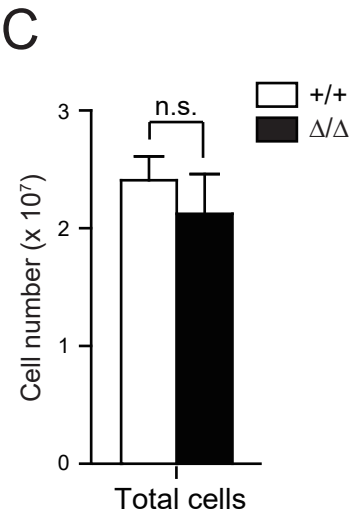
C
n.s.
+/+
Δ/Δ
Cell number (x 10⁷)
Total cells

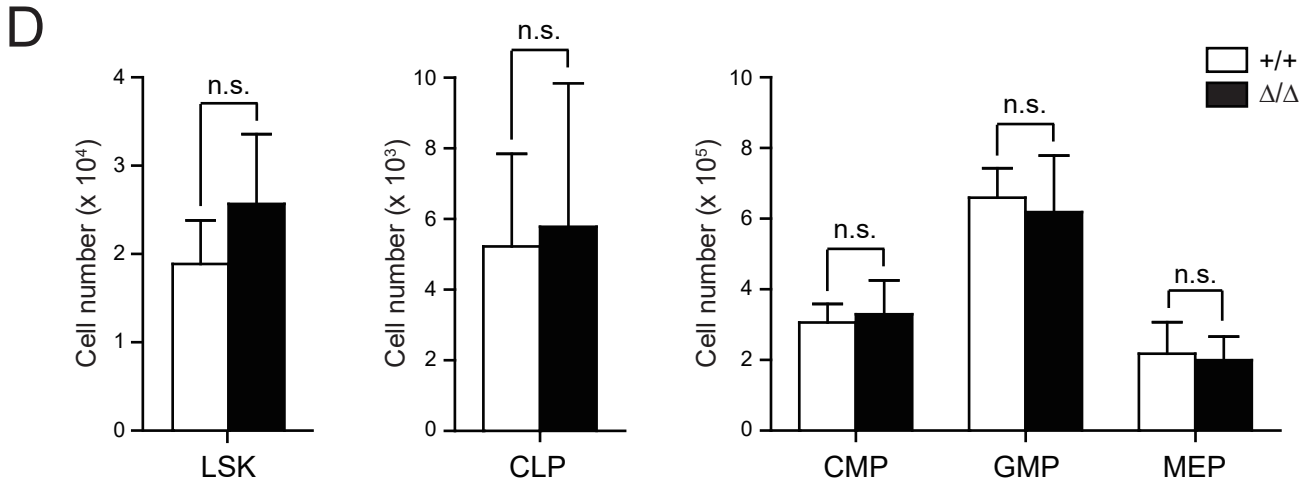
D
n.s.
Cell number (x 10⁴)
LSK
Cell number (x 10³)
CLP
Cell number (x 10⁵)
CMP
GMP
MEP
+/+
Δ/Δ

Figure 3

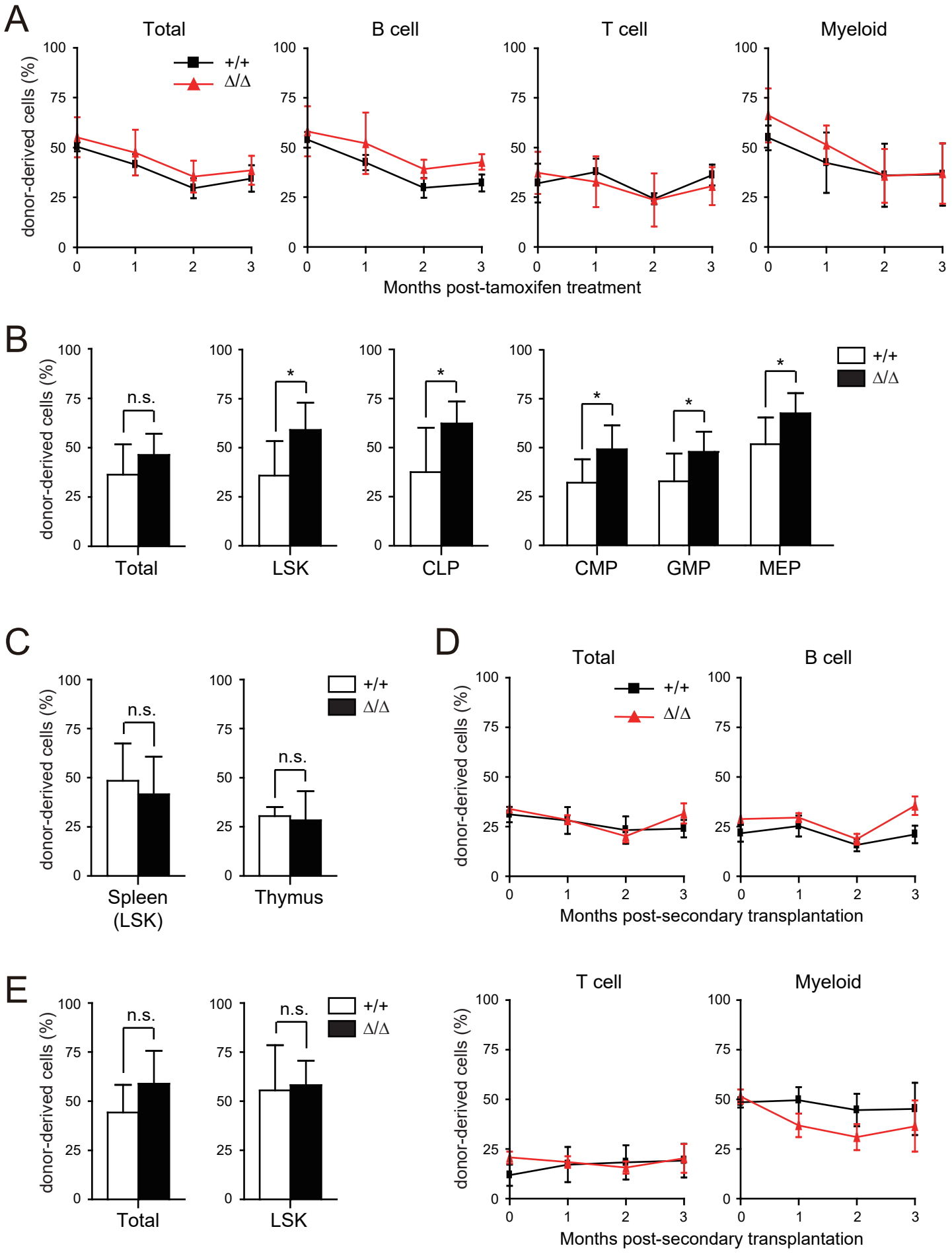
A
Total
B cell
T cell
Myeloid
+/+
Δ/Δ
donor-derived cells (%)
Months post-tamoxifen treatment
B
n.s.
*
Total
LSK
CLP
CMP
GMP
MEP
C
Spleen (LSK)
Thymus
D
Months post-secondary transplantation
E

Figure 4

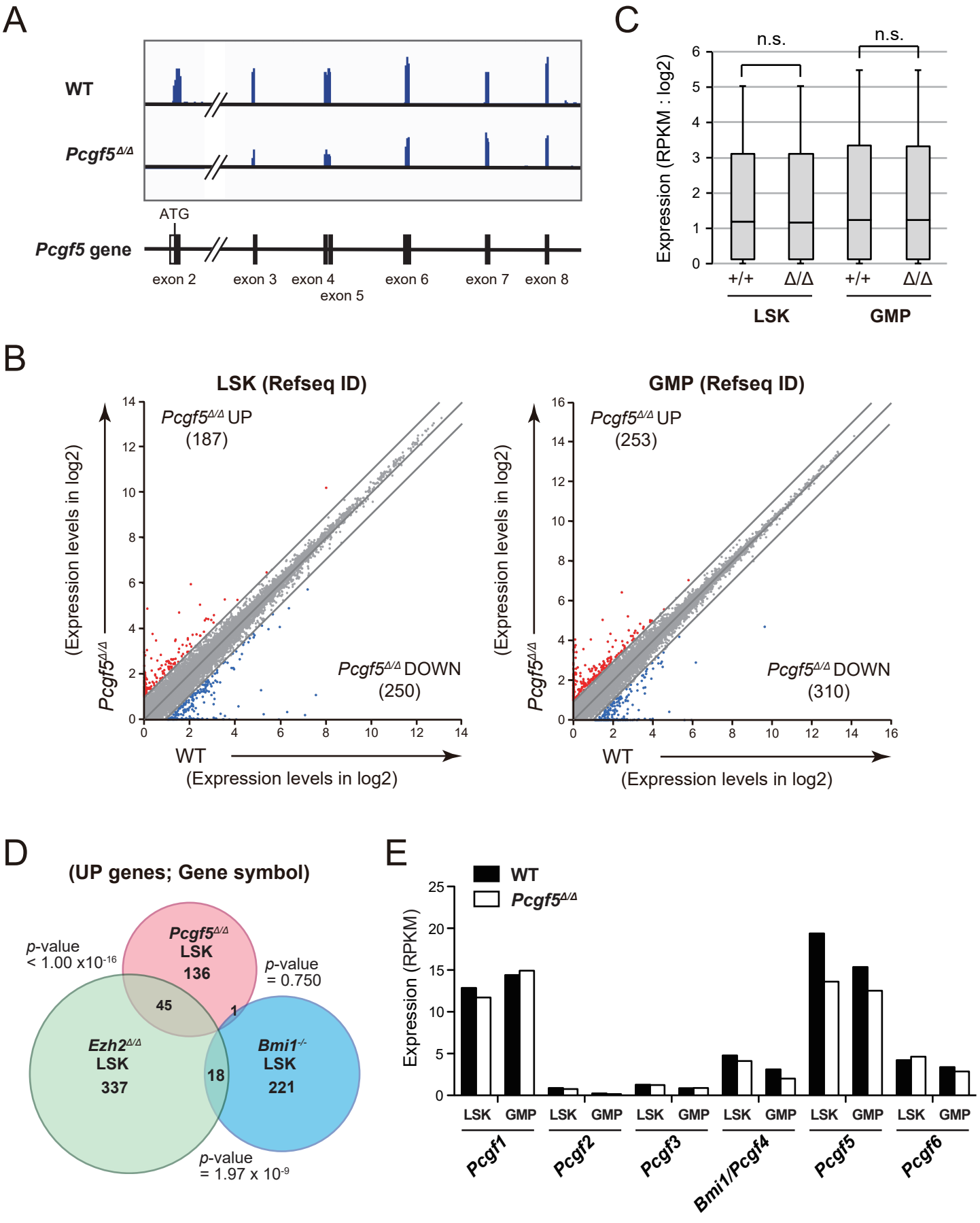
A
WT
Pcgf5Δ/Δ
ATG
Pcgf5 gene
exon 2
exon 3
exon 4
exon 5
exon 6
exon 7
exon 8
C
n.s.
n.s.
Expression (RPKM : log2)
+/+
Δ/Δ
+/+
Δ/Δ
LSK
GMP
B
LSK (Refseq ID)
Pcgf5Δ/Δ UP
(187)
Pcgf5Δ/Δ DOWN
(250)
(Expression levels in log2)
Pcgf5Δ/Δ
WT
(Expression levels in log2)
GMP (Refseq ID)
Pcgf5Δ/Δ UP
(253)
Pcgf5Δ/Δ DOWN
(310)
(Expression levels in log2)
Pcgf5Δ/Δ
WT
(Expression levels in log2)
D
(UP genes; Gene symbol)
p-value
< 1.00 x10-16
Pcgf5Δ/Δ
LSK
136
p-value
= 0.750
45
1
Ezh2Δ/Δ
LSK
337
18
Bmi1-/-
LSK
221
p-value
= 1.97 x 10-9
E
WT
Pcgf5Δ/Δ
Expression (RPKM)
LSK
GMP
Pcgf1
Pcgf2
Pcgf3
Bmi1/Pcgf4
Pcgf5
Pcgf6

Figure 5

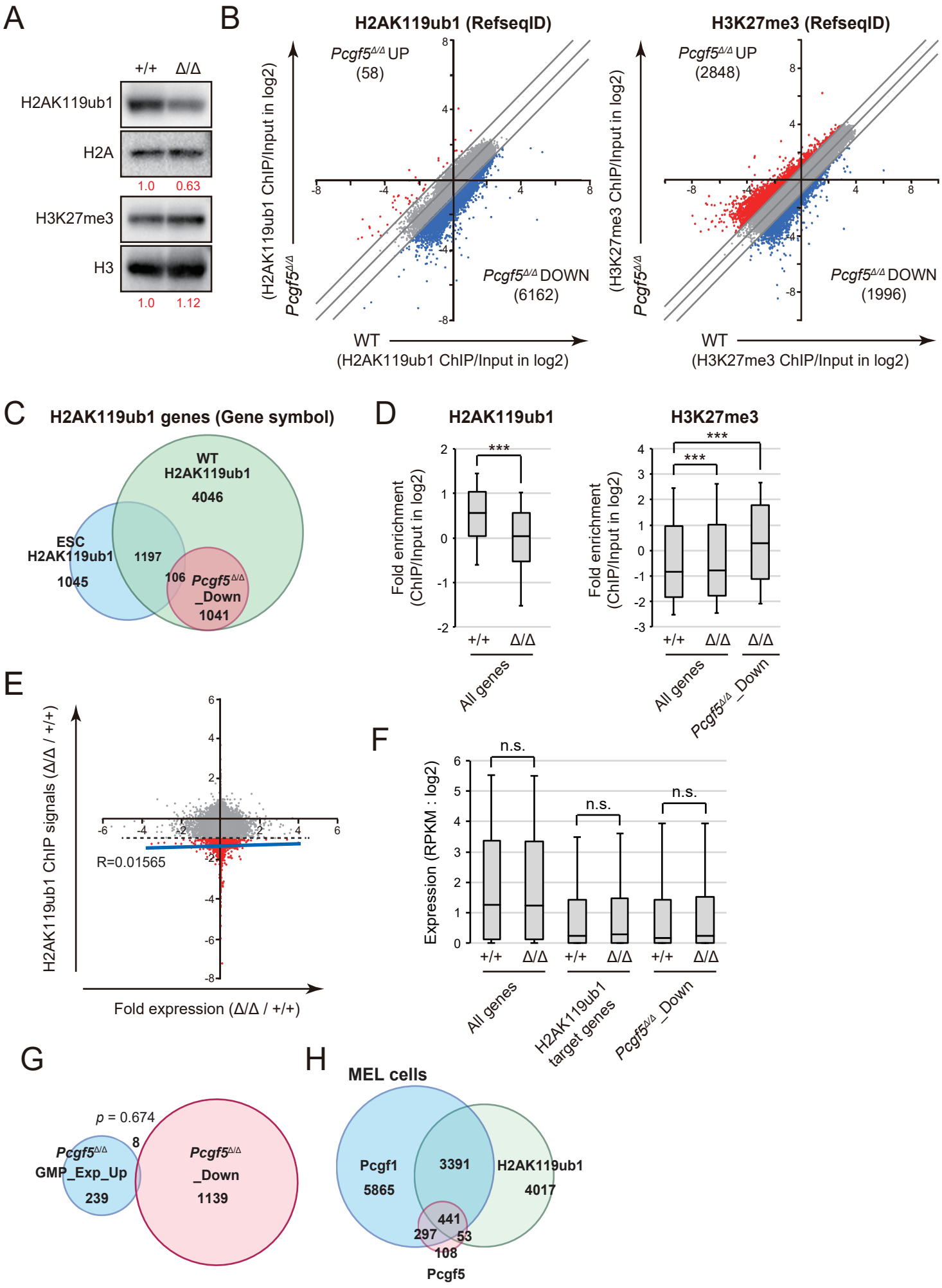
A
+/+
Δ/Δ
H2AK119ub1
H2A
1.0
0.63
H3K27me3
H3
1.0
1.12
B
H2AK119ub1 (RefseqID)
Pcgf5Δ/Δ UP
(58)
Pcgf5Δ/Δ DOWN
(6162)
(H2AK119ub1 ChIP/Input in log2)
Pcgf5Δ/Δ
WT
(H2AK119ub1 ChIP/Input in log2)
H3K27me3 (RefseqID)
Pcgf5Δ/Δ UP
(2848)
Pcgf5Δ/Δ DOWN
(1996)
(H3K27me3 ChIP/Input in log2)
Pcgf5Δ/Δ
WT
(H3K27me3 ChIP/Input in log2)
C
H2AK119ub1 genes (Gene symbol)
WT
H2AK119ub1
4046
ESC
H2AK119ub1
1045
1197
106
Pcgf5Δ/Δ
_Down
1041
D
H2AK119ub1
H3K27me3
Fold enrichment
(ChIP/Input in log2)
***
+/+
Δ/Δ
All genes
Pcgf5Δ/Δ_Down
E
H2AK119ub1 ChIP signals (Δ/Δ / +/+)
R=0.01565
Fold expression (Δ/Δ / +/+)
F
Expression (RPKM : log2)
n.s.
All genes
H2AK119ub1
target genes
Pcgf5Δ/Δ_Down
G
p = 0.674
8
Pcgf5Δ/Δ
GMP_Exp_Up
239
Pcgf5Δ/Δ
_Down
1139
H
MEL cells
Pcgf1
5865
3391
H2AK119ub1
4017
441
297
53
108
Pcgf5

Table 1

A **441 common target genes of Pcgf5 and Pcgf1 with H2AK119ub1 modification**

	Gene symbol	3xFlag-Pcgf5 /Input (log2)	3xFlag-Pcgf1 /Input (log2)	H2AK119ub1 /Input (log2)
1	Ablim1	1.28473562	1.34389186	1.89949613
2	Acap2	1.05595827	2.73995341	1.13394458
3	Ache	2.01667443	3.16507442	1.04602843
4	Adcy6	1.25500343	2.61053467	1.7905259
5	Aff1	1.46953787	3.51212962	1.24945159
6	Ago1	1.2249089	1.52006918	1.17579153
7	Agpat1	1.07325187	2.01120379	1.26323121
8	Agrn	1.00318165	2.83102786	2.66444802
9	Ak8	1.06656538	1.71776721	1.4525523
10	Alkbh5	1.06236926	2.84575464	1.35638156
11	Amd1	1.26611555	3.33079771	1.25095531
12	Amd2	1.26611555	3.33079771	1.25095531
13	Ankrd33b	1.2143872	3.55959679	1.61349671
14	Ankrd63	1.08089468	3.12477278	2.66829554
15	Anp32b	1.08039608	3.4876461	1.1018013
16	Apoo	1.32790425	1.95637727	2.17093828
17	Apoo-ps	1.26363866	1.93294196	2.12199393
18	Appl2	1.49117299	1.99275892	2.46741651
19	Arhgap21	1.57422989	4.08390851	2.02378297
20	Arhgef12	1.22337547	3.33001808	1.5032094
21	Arid1a	2.15237168	3.67288346	2.51910654
22	Arid1b	1.43097787	4.43146645	1.8038955
23	Arid2	1.63566552	4.42137296	1.18931972
24	Art4	1.58120558	1.4486516	1.2043259
25	Asic4	1.41553693	3.45119297	2.69012399
26	Ate1	1.15232572	1.92319048	1.02375563
27	Atp2b1	1.13721996	3.8399537	1.98708181
28	Atp8b2	1.2233621	2.33188043	1.67122363
29	Atxn1	1.13684536	4.2856634	1.89073725
30	B3glct	1.00288561	2.47426604	1.22980761
31	B3gnt2	1.12061015	3.18155916	1.86921407
32	B4galnt1	1.12861545	3.49545629	1.77134641
33	Bad	1.09468528	2.01600391	1.22248809
34	Bahd1	1.11485775	3.44344155	1.78087324
35	Banp	1.02657633	2.40167715	1.18639757
36	Baz2a	1.05969758	2.49165732	1.08716484
37	BB287469	1.70011037	1.03197804	1.52614754
38	Bcl2	1.2377444	3.4119319	1.87188911
39	Bcl2l11	1.03795056	3.6917661	2.23238641
40	Bcor	1.56853565	4.35159089	2.43726667
41	Brd2	1.4196688	4.30959408	1.6443342
42	Brd3	1.14721261	3.24500659	1.35638842
43	C030037D09Rik	1.08834086	3.68404867	1.41295752
44	C030039L03Rik	1.21432495	2.34661045	1.52627672
45	C330006A16Rik	1.01100742	2.63613258	1.49382983
46	C630043F03Rik	1.33207205	3.9655445	1.55139239
47	Calm1	1.16318393	3.88040954	1.81424614
48	Capn1	1.10115954	1.40092144	1.31330698
49	Cbfa2t3	1.73276644	2.05804313	1.83437677
50	Cbs	1.03860325	1.19065796	1.10940907
51	Cbx4	1.11487754	3.45244989	1.61114736
52	Ccdc63	1.14878484	1.52460785	1.73970691
53	Ccm2	1.00468897	1.87274318	1.08144853
54	Ccno	1.02904216	1.44697481	1.10485685
55	Ccrl2	1.10741079	2.19202997	1.51989435
56	Cd164	1.12202289	3.04131889	1.26321547
57	Cd24a	1.22873314	3.75150155	1.4519765
58	Cdc42ep1	1.38665794	2.983395	2.81764235
59	Cdc42ep4	1.10820885	2.83300159	1.59170735
60	Cebpb	1.25440967	3.61693192	2.17579153
61	Celsr3	1.17070853	1.75577834	1.66376532
62	Cenph	1.53310555	1.32634086	1.10940907
63	Cep55	1.00585934	1.88360374	1.14489697
64	Cited2	1.27710959	3.96201929	1.57872085
65	Clcf1	1.2945051	2.98759087	1.92426682
66	Clcn4-2	1.07595585	2.82845837	1.46739829
67	Clic1	1.22813858	2.19120556	1.48190294
68	Clip2	1.02172061	2.06166475	1.68497071
69	Cmip	1.1018692	3.04338698	1.77136323
70	Cnot6l	1.24195155	3.82390489	1.65183202
71	Cnot8	1.20230318	2.71650311	1.67834744
72	Cntfr	1.06218961	1.46189602	2.03448044
73	Cpeb2	1.32296015	4.59642563	1.86496042
74	Cpsf6	1.00318165	3.31034977	1.22509698
75	Cpt1a	1.36901439	3.4462089	1.95863975
76	Crocc	1.15555504	1.63121506	1.9208246
77	Csk	1.04083405	2.6305985	1.13398821
78	Ctbp2	1.78386009	4.7617021	2.356368
79	Ctcf	1.10115954	2.83978684	1.33794954
80	Cul4a	1.09904796	2.70462805	1.01531282
81	Cuta	1.02169684	1.7110341	1.1687775
82	Cux1	1.10863667	4.11073817	1.73781066
83	Cyb5b	1.41200842	1.58982967	1.13394595
84	D130020L05Rik	1.10820885	2.57963365	1.01533271
85	D1Ertd622e	1.41800944	3.82336275	1.53799676
86	Dcaf5	1.06815834	3.33060255	1.64583292
87	Ddost	1.39314489	1.82314425	1.03947945
88	Ddx3x	1.09670044	2.76440515	1.16365993
89	Depdc1b	1.19386819	2.2018619	1.69077671
90	Dleu2	1.12784254	3.43218394	1.22248809

	Gene symbol	3xFlag-Pcgf5 /Input (log2)	3xFlag-Pcgf1 /Input (log2)	H2AK119ub1 /Input (log2)
91	Dlx1	1.24034395	3.43959989	1.27292186
92	Dmwd	1.72724366	3.04660357	2.73884939
93	Dnajb14	1.02741427	2.70372483	1.16693737
94	Dnmt3a	1.29587212	3.56991856	2.77698728
95	Dock9	1.03700703	2.65088797	1.49654493
96	Dtnbp1	1.0921623	2.29987861	1.04322053
97	Dus3l	1.47035399	1.95203671	1.18639757
98	E130215H24Rik	1.02630432	2.89703357	1.79595039
99	Eaf1	1.1762339	2.67377273	1.07877301
100	Ece1	1.03926412	2.28416616	1.7093975
101	Eef2k	1.31387517	2.84707535	1.76298905
102	Egr3	1.40611766	3.28289607	2.05296375
103	Elf2	1.40762251	3.9685302	1.2714614
104	Erf	1.25826993	3.29970157	1.98314645
105	Espn	1.1315094	2.61689375	1.86953097
106	Etv5	1.01667443	3.62070111	1.38774602
107	F2r	1.11479373	3.045636	1.23673727
108	Fam134a	1.01236427	2.85430609	1.25135224
109	Fbxo11	1.85731905	3.50419255	1.48677587
110	Fchsd2	1.02172061	2.42055692	1.46739829
111	Fhdc1	1.2127487	3.65712303	2.31436277
112	Fli1	1.45874353	3.01831125	1.86160833
113	Flt3l	1.34285673	1.87212084	1.23673727
114	Fnbp1	1.07421641	2.37989642	1.66121835
115	Foxo3	1.16318393	4.13812755	2.53927193
116	Frmd4a	1.16471486	2.40236724	1.1687775
117	Ftl1	1.0036044	2.60233622	1.68497071
118	Fzd5	1.28473562	3.70592485	1.71573784
119	Fzd7	1.32393578	3.75590175	1.82584016
120	Gabpb1	1.18913483	3.09387894	1.52633498
121	Gadd45g	1.14728212	4.31275932	1.71185121
122	Gapdh	1.10115954	2.37864954	1.61071431
123	Gdf15	1.11485775	1.51653545	1.09693112
124	Gga1	1.05210336	1.82116425	1.22509698
125	Git2	1.22445986	3.11721197	1.62872392
126	Gm13283	1.10503547	2.40679885	1.799994
127	Gm13375	1.21129933	4.03054619	2.1018013
128	Gm15085	1.28551198	1.22514303	1.61982393
129	Gm7854	1.30919433	4.49403699	1.89783746
130	Gnas	1.34229375	3.43072039	1.59170735
131	Gpr137	1.15436947	2.05163021	1.48185204
132	Gpr146	1.02906903	2.87729494	1.69843218
133	Grb2	1.01700834	2.87992622	1.08988734
134	Grsf1	1.10578818	2.74138153	1.72554184
135	Gse1	1.83728182	4.09272536	2.86436391
136	H2afy3	1.07174549	1.40617659	1.23236749
137	H2afz	1.026926	3.17970444	1.13394769
138	H3f3a	1.26687089	3.50517209	1.04602843
139	Hes1	1.56976478	3.99907897	2.02574436
140	Hexim1	1.21918096	2.98435913	1.34044666
141	Hipk2	1.0216742	3.43889939	1.03439448
142	Hist1h1a	1.29843326	2.56274568	1.42341068
143	Hist1h2ao	1.18562204	3.89708805	1.9440222
144	Hist1h2ap	1.18562204	2.31212555	2.9440222
145	Hist1h3a	1.16471486	3.05614437	1.51067318
146	Hist1h4n	1.94786922	3.39457616	1.61948394
147	Hmga1	1.44982028	3.97345883	1.83174467
148	Hmga1-rs1	1.44982028	4.03803308	1.88400328
149	Hnrnpk	1.47738017	3.51919617	1.66671533
150	Hnrnpll	1.20945141	3.4749958	1.33985212
151	Hoxc10	1.09571871	2.4469996	1.12841068
152	Ier2	1.22588327	3.30203663	1.0888609
153	Ifngr2	1.54485903	2.61691328	1.78087324
154	Igf1r	2.09028889	4.67122438	2.28592505
155	Inafm1	1.19455557	2.40236724	1.24528306
156	Ints6	1.55461402	3.23475981	1.12500594
157	Iqce	1.18886004	2.33425797	1.38875494
158	Irf2bp2	1.3660269	4.05163021	1.89398471
159	Irgq	1.49866613	2.65480874	1.99682881
160	Irs2	1.18913483	4.34033988	2.09695348
161	Itpk1	1.31387517	2.51185634	2.11130138
162	Jade1	1.18171702	3.33529451	2.09695348
163	Jade2	1.71613941	3.32146177	1.55429558
164	Josd1	1.12725674	3.01467689	1.21548333
165	Junb	1.20760438	3.82616559	1.70866079
166	Jund	1.00694265	3.42472968	1.09327997
167	Kazald1	1.04083405	3.42102207	1.7188881
168	Kcne3	1.10254344	2.15598199	1.49382983
169	Kdm5b	1.00585934	3.28829011	1.78930119
170	Keap1	1.00169512	2.69266413	1.47601157
171	Kifc1	1.25619346	1.13763924	1.35638842
172	Klf1	1.21223011	2.46666388	1.4906974
173	Klf10	1.61734274	3.65759909	1.81089619
174	Klf13	1.36462611	4.08500916	1.42429605
175	Klf16	1.01178796	2.76827532	2.0807268
176	Klhl17	1.1725219	3.0282395	1.48677587
177	Klhl22	1.14723853	2.89699687	1.59732752
178	Kmt2a	1.65675427	3.49866006	2.00544341
179	Kmt2c	1.3387067	3.78912743	1.0418135
180	Kmt2e	1.18957335	3.22462734	1.02700775

	Gene symbol	3xFlag-Pcgf5 /Input (log2)	3xFlag-Pcgf1 /Input (log2)	H2AK119ub1 /Input (log2)
181	L3mbtl3	1.15436947	3.45763675	1.06684201
182	Lemd3	1.05128964	3.17374368	1.70573431
183	Lgr5	1.7301972	1.70646506	3.72424161
184	Lincpint	1.02169319	3.11747813	1.4323351
185	Lmnb1	1.0216742	3.57858164	1.33867973
186	Lpcat4	1.44522637	2.6305985	1.37651228
187	Lphn1	1.22813858	3.1942393	1.87901021
188	Lrrc59	1.01182513	3.20825101	1.14613045
189	Lrrc8d	1.12391929	3.60131477	1.69338472
190	Ltk	1.50718346	2.83702821	1.25095531
191	Lyl1	1.48660137	2.2280565	2.41477982
192	Maml3	1.09294514	3.88279364	1.20825217
193	Man1a2	1.01663691	3.326692	1.00101091
194	Man2a1	1.10367084	3.39854107	1.68609291
195	Mapk14	1.00235054	3.47257062	1.63547242
196	Marcksl1	1.02170305	2.75065299	2.28929058
197	Mars2	1.02172938	2.65986402	1.42845936
198	Maz	1.33298861	3.32475266	2.00646813
199	Mb21d1	1.24229853	3.03407809	1.71308982
200	Mbnl1	1.11085287	2.44182904	1.54273921
201	Mbp	1.06595583	2.36152036	1.35636956
202	Med13l	1.25374485	3.93711618	1.8969468
203	Mesdc1	1.12861545	3.70812915	1.94131422
204	Mettl6	1.18216602	2.71336332	1.04322053
205	Mex3b	1.10032246	4.25390447	2.11130138
206	Mfsd11	1.24034395	3.02591202	1.07347244
207	Mfsd2b	1.09971784	1.74331736	1.56933297
208	Micall2	1.32126993	1.93610885	2.04183242
209	Mid1ip1	1.12944262	3.02110727	1.28680826
210	Mief2	1.01100742	2.46604948	1.21193482
211	Mir5135	1.10946878	3.03054619	2.18353196
212	Mir5620	1.04560875	2.8005579	1.67000563
213	Mir6236	2.13072245	1.97276604	1.07089986
214	Mir7687	1.43228905	3.60971353	2.70918912
215	Mir7b	1.31651903	1.1981645	1.40879585
216	Mir8105	1.08039608	2.49010807	1.3742322
217	Mllt3	1.15436947	3.36853701	1.57354924
218	Mnt	1.18518958	3.18041107	1.52635255
219	Mpzl2	1.6173882	1.75065299	1.73781066
220	Mrpl12	1.05595827	1.742471	1.3265633
221	Msi2	1.26538494	3.5380497	1.3563391
222	Mvb12b	1.00468897	2.24153967	1.31687365
223	Myb	1.01700834	3.54073347	1.35635012
224	Myc	1.8055739	3.68025647	1.4906974
225	Myh10	1.24871938	2.99254639	1.67830245
226	Mylip	1.07635862	3.47565109	1.16109646
227	Naf1	1.77513579	2.36758703	1.19591495
228	Nckap1	1.62380601	3.90076994	1.21016446
229	Ncor2	1.21171651	2.89095145	1.94127141
230	Ndst2	1.31760009	2.20411228	1.49382983
231	Nfat5	1.20678601	2.64698691	1.14293835
232	Nfatc4	1.00318165	2.08970411	2.07694885
233	Nfe2l2	1.23416471	3.41933315	1.01928975
234	Nfia	1.08039608	3.51000282	2.11637713
235	Noc2l	1.09468528	3.01228549	1.42429605
236	Nol4l	1.3350277	3.98254255	2.67824247
237	Nop56	1.05345294	1.8374101	1.05052358
238	Npas4	2.69981446	2.91319977	2.09327997
239	Nr2f1	1.16219458	3.81664945	1.11127405
240	Nr2f6	1.04085847	2.45072133	1.40215994
241	Nt5c2	1.20120873	2.42710079	1.72339681
242	Oaf	1.44762306	2.85646291	1.39239031
243	Orai3	1.04936713	2.17950264	1.35632832
244	Ott	1.28551198	1.22514303	1.61982393
245	Oxsr1	1.14228116	2.4267381	1.28680826
246	Pabpc4	1.01392029	1.62451772	1.13394595
247	Paip1	1.14723853	3.7319671	1.57459059
248	Paqr7	1.10311847	2.41966003	1.60251981
249	Parl	1.12511329	1.38752973	1.11280489
250	Pawr	1.12784254	3.36649923	1.356368
251	Pax6	1.54485903	3.59049332	1.86537628
252	Pbx2	1.05210336	2.48760679	1.50995893
253	Pbx3	1.1851903	3.12717463	1.62872392
254	Pcid2	1.10414503	2.66321653	1.05052358
255	Pde3b	1.026926	3.78903787	1.73189065
256	Pde4a	1.15808239	3.0251245	1.72790085
257	Pfn1	1.33417137	3.57823336	1.05677277
258	Pgls	1.3928401	2.47772686	1.16756223
259	Pgpep1	1.14908432	1.96799138	1.76727161
260	Phf12	1.00694265	2.82692705	1.0608406
261	Phf13	1.42026503	3.72255783	2.80886003
262	Phf21a	1.25374485	3.33749935	1.10483342
263	Pim3	1.03857097	3.39881685	1.87419582
264	Pip4k2a	1.20380964	3.0857091	1.25323526
265	Pkd1l2	1.62180069	1.72075317	2.22310676
266	Plec	1.06907329	2.45489297	2.21963306
267	Plekhh3	1.54230268	3.06290648	2.83443932
268	Plxnc1	1.3350277	3.92025936	2.50200566
269	Pnpla7	1.14721261	2.04873028	1.5262248
270	Poldip3	1.19216926	2.81692591	1.46496092

	Gene symbol	3xFlag-Pcgf5 /Input (log2)	3xFlag-Pcgf1 /Input (log2)	H2AK119ub1 /Input (log2)
271	Pou4f1	1.12432504	3.52511509	1.19717845
272	Ppargc1b	1.3747085	3.16179999	1.27837531
273	Ppp1r3f	1.04218674	2.16233195	1.11821096
274	Ppp1r3fos	1.00792152	2.38732477	1.24472047
275	Prkab1	1.26611555	2.91223053	1.3742322
276	Psat1	1.31870136	2.65326553	1.61940397
277	Psma7	1.31515971	2.64516621	1.4525523
278	Psmb3	1.00694265	2.62378418	1.45304313
279	Ptch1	1.62422662	4.14297509	2.08988734
280	Ptma	1.60671842	3.82239101	1.76298905
281	Ptprs	1.43679359	2.59809821	2.56826763
282	Ptpru	1.12202289	3.77235272	2.16368335
283	Pxk	1.28474405	2.34245404	1.19131668
284	Rai1	1.55782731	3.38158693	1.53322108
285	Ranbp1	1.1378923	2.58399368	1.24085716
286	Rap1b	1.00585934	2.95640576	1.48196741
287	Rarg	1.06540646	3.4991115	2.30187794
288	Rasa3	1.50717599	2.71314376	1.03439448
289	Rasal1	1.26812006	2.09219854	2.22146021
290	Rbbp4	1.07417614	2.35605442	1.22861029
291	Rcor1	1.36135557	3.61694464	1.80805339
292	Rdm1	1.17368238	2.27902741	1.11541758
293	Reep5	1.17847747	2.47254231	1.19811303
294	Rhob	1.10920714	3.72442807	2.13394595
295	Rhoq	1.03587187	2.98793812	1.80697098
296	Rmi1	1.55461402	3.46030936	1.71251307
297	Rnasek	1.03587187	2.48415629	1.1637096
298	Rnaset2b	1.15931032	1.96708416	2.52631155
299	Rnpepl1	1.03986049	3.03837961	2.17450696
300	Rnu12	1.13907775	2.81703891	1.3090222
301	Rogdi	1.16379105	1.80960456	1.76378811
302	Rpl29	1.10503547	1.09341502	1.10485685
303	Rpl31	1.06595583	1.99718831	1.11532068
304	Rsrp1	1.02657633	3.49220133	1.29557131
305	Rtbdn	1.63510721	2.35474074	2.18236636
306	Runx1	1.10414503	1.51282854	1.05551441
307	Rxrb	1.18131261	2.31332729	1.81424614
308	S1pr1	2.16446841	2.69024906	2.27386765
309	Samd11	1.61237677	2.60312332	1.94134905
310	Sap30	1.06595583	2.85395467	1.15471703
311	Schip1	1.08089468	3.7079747	1.97449473
312	Scrib	1.13370566	1.8095828	1.29747557
313	Scrt1	2.30095624	3.28404205	2.29423615
314	Senp6	1.30550752	3.51967879	1.60568032
315	Serf2	1.18528358	2.78533164	1.22858296
316	Setd1a	1.02172061	2.19951597	1.25950466
317	Setd1b	1.12861545	2.930298	1.51989435
318	Sgms1	1.09754735	3.33529451	2.26712678
319	Sgsh	1.43062848	1.84985613	2.8054126
320	Shb	1.37784748	3.59174237	2.18525771
321	Shox2	1.11481905	3.6763286	1.16371129
322	Siah2	1.03535812	3.58011361	1.67340462
323	Six2	1.18528358	3.10549833	1.65589466
324	Six5	1.03795056	3.18999515	1.75372634
325	Ski	1.30311842	3.6543072	2.52630561
326	Skil	1.45756405	3.59293073	1.67824247
327	Slc14a1	1.1880674	1.88758862	1.24472047
328	Slc16a13	1.17184765	1.83813373	1.74630021
329	Slc16a6	1.0459464	3.34245404	1.47664512
330	Slc26a11	1.41200842	1.82285303	2.76934857
331	Slc35b2	1.2205981	2.03605269	1.25167783
332	Slc38a7	1.24722893	1.15951021	1.90476654
333	Slc39a7	1.27532446	2.36416538	1.77577759
334	Slc48a1	1.15547357	2.74304904	1.05197966
335	Smad7	1.22652898	4.2932214	1.83594763
336	Smarcc2	1.0009544	2.48161862	1.25323526
337	Smarcd2	1.18853026	2.42294724	1.28137358
338	Smek1	1.12162841	2.45431839	1.1438524
339	Sms	1.09062404	2.76732188	1.45941465
340	Snca	1.21432495	1.75186888	1.025722
341	Snora16a	1.07174549	1.90387556	1.55665223
342	Snord110	1.41971602	1.8465757	1.28923332
343	Socs2	1.05735574	3.78533164	1.97881187
344	Spred1	1.06907329	3.85299727	1.67824247
345	Spred2	1.10115954	3.36287787	1.43882593
346	Sptbn4	1.52701327	1.95121126	1.7245205
347	Srsf1	1.31870136	3.15493159	1.17265174
348	Ss18l1	1.31515971	2.64516621	1.46924114
349	Ssbp4	1.12092624	2.90716023	1.73781066
350	St3gal4	1.10695505	2.35780081	1.61939897
351	Stk40	1.55125351	2.56802097	1.6537769
352	Stt3b	1.05998875	3.35016759	1.0608406
353	Stx2	1.14340174	2.00686868	1.28137358
354	Tal1	1.72676124	3.69838802	1.65589466
355	Tfap4	1.69981446	3.09384779	1.45609
356	Tfe3	1.13721996	2.04520285	1.78927881
357	Tfeb	1.02784986	2.61383078	1.66571669
358	Tfr2	1.53628728	1.72707943	2.01008071
359	Tgif1	1.60491319	3.34281463	1.64759457
360	Tgif2	1.16632605	2.83506895	2.06686544

	Gene symbol	3xFlag-Pcgf5 /Input (log2)	3xFlag-Pcgf1 /Input (log2)	H2AK119ub1 /Input (log2)
361	Them6	1.10695505	2.82875923	1.14293835
362	Tiparp	1.07258104	4.06995263	1.30084089
363	Tle1	1.2042609	3.96941594	1.61941596
364	Tmem14c	1.3587631	2.02886325	1.14985593
365	Tmem206	1.03587187	1.99673916	1.61071431
366	Tmem88	1.03689447	1.32145413	1.3563391
367	Tnk2	1.03323296	3.16439353	1.83941155
368	Tnpo2	1.47966249	2.38773423	1.45587404
369	Tnrc6c	1.1378923	4.29116874	2.25097767
370	Trim16	1.03795056	2.24740604	1.22248809
371	Trim8	1.53475679	3.98356322	1.4465302
372	Trmt2a	1.04770912	2.57843076	1.26888863
373	Trp53	1.32273198	2.45431839	1.13394595
374	Tsc22d2	1.3093064	4.11313526	1.36811428
375	Tsc22d3	1.03238627	3.47515041	1.2204258
376	Tsc22d4	1.12861545	2.79011067	1.42194178
377	Tshz1	1.14411776	4.28570611	2.03755824
378	Tspan32	1.98273489	1.73662838	1.4861253
379	Ttyh2	1.08089468	2.80175511	1.57872085
380	Tyro3	1.21720727	2.65619181	1.46428644
381	Ubald1	1.14344857	3.12084143	1.63475097
382	Ubr3	1.08678532	2.76203476	1.30185902
383	Ubr5	1.07829063	2.54373984	1.2042967
384	Ubtf	1.46534275	4.3747573	1.97783505
385	Unkl	1.1148678	2.27833575	1.08571266
386	Usf2	1.01667443	2.42731858	1.41520806
387	Usp49	1.06540646	1.82974433	1.13398821
388	Usp7	1.05932941	3.45072133	1.94128407
389	Vars	1.47356136	2.67117531	1.69349176
390	Vdac1	1.24340676	3.05617685	1.73189065
391	Vegfa	1.16794346	3.62788109	1.8344267
392	Vezf1	1.15668789	2.75209969	1.60251981
393	Vgf	1.03418085	2.53688765	2.74574742
394	Vim	1.56229797	3.24421613	1.70783166
395	Vstm2l	2.10695505	2.34245404	1.23673727
396	Wdr26	1.02784986	2.75709695	1.35638156
397	Wipf2	1.29699449	1.96432255	1.08988734
398	Wnt5b	1.23865965	1.23103206	2.14221853
399	Wrap53	1.01700834	2.10650978	1.42940688
400	Xkr7	1.09062404	1.22459207	1.42284159
401	Xylt1	1.00908349	2.99089645	1.65589466
402	Yipf6	1.13271291	2.66041802	1.49396797
403	Ywhaz	1.41596644	3.41138043	1.39484427
404	Yy1	1.21437235	3.42915343	1.69344596
405	Zadh2	1.10367084	3.70902919	1.67828446
406	Zbtb25	1.19806824	3.85460585	1.61941596
407	Zbtb7a	1.07830799	3.82996579	1.32466941
408	Zbtb8os	1.15746458	2.35093941	1.17836549
409	Zc3hav1	1.00065072	3.45343431	1.87318946
410	Zdhhc17	1.08039608	3.31481394	1.53192304
411	Zdhhc2	1.18040841	2.71287998	1.05383104
412	Zeb2	1.24034395	3.91624117	1.57869743
413	Zfand5	1.03587187	3.58867702	1.2699241
414	Zfp36l1	1.17936516	3.80608438	1.49382983
415	Zfp36l2	1.35035291	4.84399504	2.37945841
416	Zfp609	1.04218674	2.59736952	1.3774425
417	Zfp703	1.09102625	3.86959618	1.35636221
418	Zfp768	1.07177847	1.66197808	1.10260439
419	Zfp821	1.27487142	2.6997772	1.4906974
420	Zfpm1	1.41437934	2.94593843	2.15471703
421	Zic5	1.32126993	3.27391439	1.21888719
422	Zmiz1	1.65754354	4.76262572	2.09327997
423	Zmym3	1.14736814	1.92154248	1.03435348
424	Zmynd11	1.62422662	3.68962453	1.29493094
425	Znrf1	1.02741427	2.47701504	1.32354066
426	8-Sep	1.15727929	2.80958489	1.40700722
427	0610010K14Rik	1.03587187	2.87257165	1.84616878
428	2410004B18Rik	1.11485775	2.37107734	2.03695161
429	2610005L07Rik	2.10194731	2.2766976	1.26330994
430	2700046G09Rik	1.29381403	3.46666532	1.87094753
431	4930426L09Rik	1.26687089	2.97005506	1.23236749
432	4930581F22Rik	1.00318165	2.33079771	1.58226983
433	4931440J10Rik	1.46009803	3.21732878	1.25095531
434	4931440P22Rik	1.05649024	3.89606313	1.10991697
435	5430405H02Rik	1.02841506	3.21646119	1.89241605
436	5730420D15Rik	1.01726781	3.8726275	1.35631437
437	5830417I10Rik	1.59288439	1.75291063	1.06696582
438	6530402F18Rik	1.08977315	3.73353056	1.99646205
439	9530052E02Rik	1.16632605	4.20793972	2.32723923
440	9630033F20Rik	1.26687089	1.27088409	2.18639757
441	A530013C23Rik	1.17847747	3.44784394	2.04563319

B **53 Pcgf5 target genes with H2AK119ub1 modification, but not bound by Pcgf1**

	Gene symbol	3xFlag-Pcgf5 /Input (log2)	H2AK119ub1 /Input (log2)
1	Apba2	1.380618855	1.166326048
2	Ar	1.356281576	1.056490239
3	Ascl2	1.299763145	1.534756795
4	Bhlhe41	1.175791527	1.163183929
5	Cda	1.278367461	1.3350277
6	Crb2	1.481902938	1.13684536
7	Dlk1	1.558913326	1.309306398
8	Dner	1.267558406	1.144117756
9	Dpysl3	1.240927595	1.078307993
10	Epo	1.157045168	1.092945136
11	G530011O06Rik	1.467325403	1.635665522
12	Gm11236	1.357798051	1.449820276
13	Gm11237	1.357798051	1.072581041
14	Gm1140	1.356537505	1.21129933
15	Gm14692	1.356537505	1.569764781
16	Gm15133	1.357798051	2.090288885
17	Gm1604b	1.204786433	1.309194333
18	Helt	1.407007218	1.137219963
19	Hhex	1.408795851	1.017267808
20	Hspb1	1.672785994	1.624226618
21	Idi2	1.093279969	1.3350277
22	Il3ra	1.074533799	1.204260903
23	Ipw	1.482182937	1.568535652
24	Kcna6	1.503209399	1.100322461
25	Lhx1	1.249451586	1.091026248
26	Lhx1os	1.182296492	1.623806012
27	LOC100862015	1.357798051	1.366026899
28	LOC101055863	1.357798051	1.226528977
29	LOC102636514	1.672785994	1.240343954
30	Mir6538	1.414092412	1.207604376
31	Mir6988	1.55085067	1.837281816
32	Mybpc3	1.963984652	1.198068236
33	Nhlrc4	2.263204971	1.277109591
34	Nkd1	1.340922655	1.069073291
35	Nxph1	1.521024691	1.332072053
36	Ophn1	1.69736165	1.322960154
37	Pappa	1.146130449	1.449820276
38	Pirb	2.678662407	1.137892299
39	Podn	1.83594763	1.185622041
40	Prkcdbp	1.412957516	1.465342748
41	Psme1	1.005443411	1.574229888
42	Pvrl4	1.372443476	1.25374485
43	Rpp25	2.178365489	1.364626113
44	Scgb1b29	1.357798051	1.350352913
45	Slc4a1	2.921477549	1.657543542
46	Snord116	2.94781378	1.419668797
47	Snord116l1	2.94781378	1.147282122
48	Snord116l2	2.94781378	1.189134832
49	Sytl3	1.760754028	1.430977868
50	Tmem86b	1.655035072	1.407622508
51	Trim12a	1.357798051	1.783860089
52	Tspo2	1.376512284	1.108636675
53	4931431F19Rik	1.115320683	1.163183929

PLoS One, 11(5):e0154561
平成28年5月2日　公表済